Computer Simulation Of A Complete Microwave Radiometer System

Skou, Niels; Kristensen, Steen Savstrup; Gudmandsen, Preben

Published in:
Geoscience and Remote Sensing Symposium

Publication date:
1990

Document Version
Publisher's PDF, also known as Version of record

COMPUTER SIMULATION OF A COMPLETE MICROWAVE RADIOMETER SYSTEM

N. Skou, S. S. Kristensen, and P. Gudmandsen

Technical University of Denmark
B 348, DK 2800, Lyngby, Denmark

ABSTRACT

A computerized tool for simulating the performance of a complete imaging microwave radiometer system has been developed at the Electromagnetics Institute. The input to the simulator is a two dimensional brightness temperature scene, and the output is an image including the artifacts introduced by the simulated instrument. The computer program simulates the antenna convolution and the spatial smearing of the integrator. It adds radiometer noise, and takes into account gain and calibration instabilities. Finally, it makes a linear spatial deconvolution of the antenna directivity pattern.

Key words: Radiometer, microwave, simulation.

INTRODUCTION

Spaceborne and airborne imaging microwave radiometers are complex systems, and although design guidelines can be found in for example [1], [2], and [3] it is not easy to get an overview of the final performance of a given system. Especially regarding spaceborne systems this is not satisfactory as there is no way of making modifications once the system has been launched.

An ideal radiometer system would measure a given brightness temperature scenario with no errors. A real radiometer system introduces errors, that can be divided into two major catagories: antenna measurement errors and radiometer receiver errors.

The purpose of the antenna is to collect the emitted energy from a target and present it to the input of the radiometer. The ideal antenna has a pencil beam with high gain in one direction and zero gain in all other directions. The realistic antenna has a relatively broad main lobe and sidelobes. When measuring the brightness temperature of a given ground element in the main lobe, the antenna thus picks up significant power from neighbouring elements through the broad main lobe, and even from quite distant elements through the sidelobes. This may result in significant measurement errors. In an imaging system the antenna footprint moves across the scene to be sensed, and that process corresponds to a convolution of the antenna pattern with the brightness temperature distribution of the scene. Hence, the spectrum of the scene is multiplied with the transfer function of the antenna (the Fourier transform of the antenna pattern) resulting in measurement errors: gradients in the scene are smoothed. Finally the antenna output has to be measured at certain time intervals (sampling) and hence aliasing may result.

The purpose of the radiometer is to measure the output from the antenna. The ideal radiometer selects a certain bandwidth of the available antenna signal, amplifies and detects the signal and presents the result to a certain output device - typically an A/D converter. The response time of the ideal radiometer is very fast. In a real radiometer bandwidth, gains, and offsets may change with time, temperature, and supply voltages resulting in measurement errors. A real radiometer generates noise. As the antenna signal is also a noise signal and the two signals are independent, they will add and cannot later be separated again. The real radiometer needs a certain integration time, resulting in a transfer function that must be added to the antenna transfer function to find the system response to varying input signals. The result is further smearing of the input scene in the scan direction.

All these effects can be evaluated using the computer simulator described in the following.

THE SIMULATOR

The computerized simulator is primarily intended for evaluation of a millimeter wave sounder embarked on a geostationary satellite wherefrom it scans the Earth disk or parts thereof. This means that many features of the simulator are especially tailored for that purpose (scan geometry, receiver type, test scenes, a. o.). However, this does not preclude the simulation of many features of general nature - common to all imaging radiometer systems.

The input to the simulator is a two dimensional apparent brightness temperature scene to be scanned by the antenna, and the output is a two dimentional image.The brightness temperature dependence on geophysical parameters is not part of the simulater.

CH2825-8/90/0000-01577/$01.00

The input brightness temperatures may be provided in a data file or may be synthesized using analytical functions inherent in the simulator. Thus simple test patterns composed of linear, sinus, and square wave functions of the two dimensions are readily at hand.

The simulation process is divided into three phases:

Phase 1 concerns the antenna, and simulates the antenna scanning, the antenna convolution, and the smearing effect of the radiometer's integrator. The antenna is assumed to have rotationally symmetric pattern, and its shape can be provided in a data file, or synthesized internally using either $|J_1(x)/x|$ or $|\sin(x)/x|$ raised to powers typically between 2 and 5. Scanning parameters like distance between scan lines, scan speed, and sampling distance is entered. The spatial smearing effect of the integrator is performed as a convolution in the scan direction of the input scene and the spatial response function of the integrator. This is done before the antenna convolution in order to save computing time.

Phase 2 concerns the radiometer receiver and the calibration hardware. First of all noise is added, thus simulating the radiometer's ΔT. Secondly, calibration targets, gains, losses, bandwidths, and offsets associated with typical radiometer subsystems can be given their nominal values, a fluctuation term, and temperature dependence. A range of thermal scenaria can be implemented. The calibration scheme is defined. Based on all this the simulator calculates the antenna temperature as estimated by the radiometer.

In phase 3 a linear spatial deconvolution of the antenna directivity pattern is performed, taking into account the spatial power spectrum of both the apparent brightness temperature and the instrument errors. The deconvolution follows [4] with the modifications that the brightness temperature is taken as input and that only one channel is considered at a time.

Any of the above described steps in the simulation process can be by-passed to speed up the computations. If, for example, we are interested in the antenna convolution and deconvolution alone, the simulation of the radiometer reciever can be greatly simplified to account only for radiometric noise.

EXAMPLES

In the following three examples of simulations will be presented. The examples concern features of general nature within imaging microwave radiometer systems. The examples are designed so, that they can be illustrated by one dimensional graphs, but the simulations are truely two dimensional and the graphs are one dimensional cuts in the output image.

ERRORS DUE TO ANTENNA PATTERN

A typical antenna pattern to be used in the following is shown in **Figure 1**. $|J_1(x)/x|^{3.2}$ has been found to resemble the patterns of many imaging systems well. Only the two first sidelobes are considered here as the rest give negligible contribution.

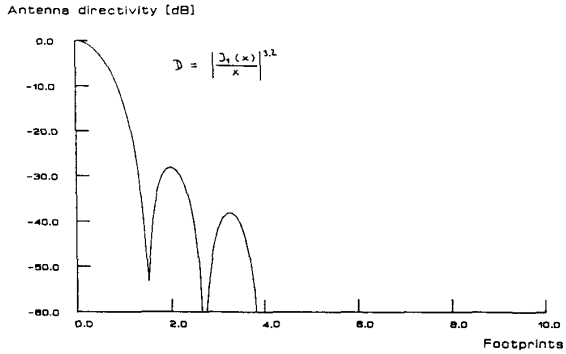

Figure 1: Typical antenna pattern

In **Figure 2** this pattern sweeps across a scene with large contrasts in the scan direction (uniform in the orthogonal direction). The square wave curve is the cut through the scene, while the smoothed curve shows the result after antenna convolution. It is clear that around the contrast points the antenna response cannot follow the scene, resulting in measurement errors. The RMS error across the whole scene is calculated by the simulator to be 1.41 K. If we are designing a system with a radiometric resolution of say 0.5 K, such scenes give rise to concern.

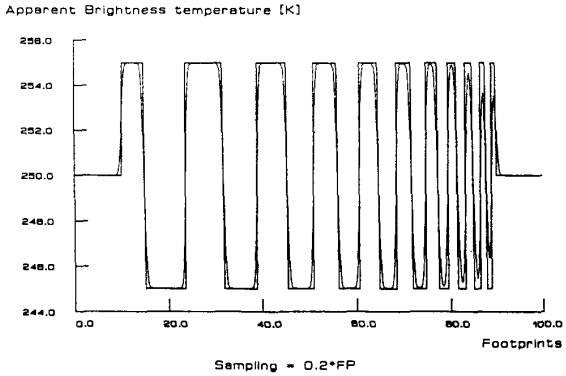

Figure 2: Scene with large contrasts being smoothed by the antenna

ALIASING ERRORS

In the past it has been discussed which sampling rate to use in imaging radiometer systems in order to avoid excessive aliasing. Some claim that sampling twice per 3 dB footprint is required, while systems

having only sampling once per footprint have been operated successfully (SMMR). In [2] it is claimed that a reasonable compromise is between these two figures, namely a sampling interval of 0.7 footprints. In [5] it is attempted to calculate the amount of aliasing analytically. The result is that a sampling interval of some 0.5 footprints is needed, but this corresponds to a worst-worst case due to a rather crude assumption about the spectral density of the ground scene being imaged. The simulator can directly assess the level of aliasing for selected scenes and sampling rates.

Figure 3 shows a square wave test pattern with 10 K peaks (actually ridges in the two dimensional input scene) that are from 2 to 1/2 footprints wide. Again our typical antenna pattern sweeps across the pattern, and the smoothed result is also shown in the figure. Note the large measurement errors as the peaks become narrow compared with the footprint.

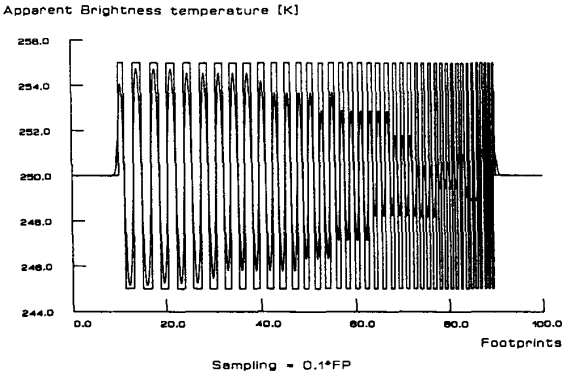

Figure 3: Scene used to evaluate aliasing

Aliasing errors for sampling intervals of 0.5, 0.7,and 1.0 times the footprint are shown in **Figures 4 to 6.** As expected there are practically no errors for 0.5 footprint sampling and large errors for a 1.0 footprint interval. For 0.7 footprint sampling interval the RMS aliasing error over the total scene (Figure 5) is calculated by the simulator to be 0.165 K. Note that the dominating error is around footprint no. 80 where the scene peaks are less than 1 footprint wide and where the measurement data are useless anyway, see Figure 3. The peak error is estimated to 0.53 K. The scene has an RMS value of 5 K. According to [5] this value will give a worst case aliasing error of 0.5 K in good agreement with our results. The general error in Figure 5 (excluding the peak error) is estimated to be 0.07 K, so if the present case for example concerns a radiometer system with a ΔT=0.5 K, a sampling interval of 0.7 footprints seems fine.

DECONVOLUTION

Figure 7 shows a test pattern (square wave curve), the antenna response (smooth, rounded curve), and the result after deconvolution in the ideal case where

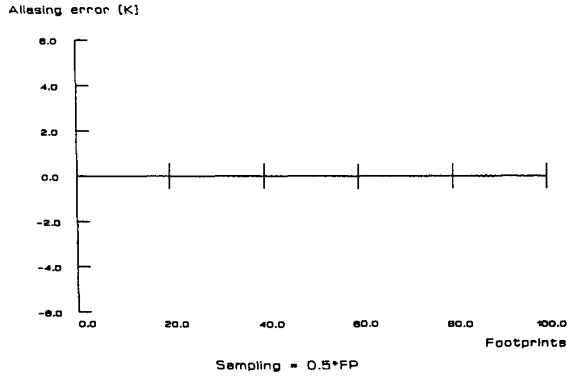

Figure 4: Aliasing error for 0.5 footprint sampling

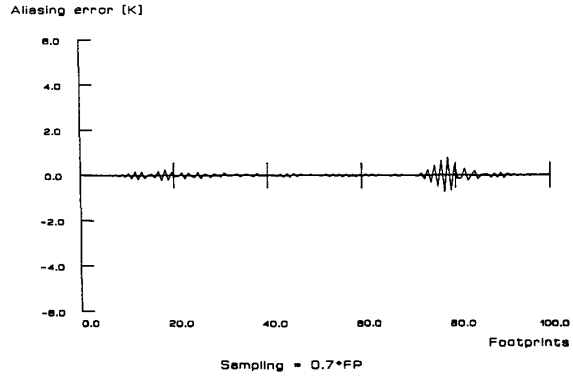

Figure 5: Aliasing error for 0.7 footprint sampling

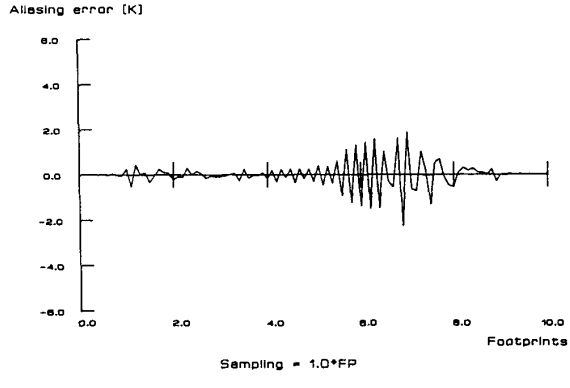

Figure 6: Aliasing error for 1.0 footprint sampling

the radiometric noise ΔT is zero. The deconvoluted curve shows better ability to follow the steep jumps in the test pattern - but overshoots due to lack of the highest frequencies in the scene spectrum after antenna convolution. The antenna convolution process is in effect a low pass filtering, the higher frequencies in the input scene are attenuated and above a certain cut-off frequency they are effectively

nullified. The deconvolution process tries to amplify the attenuated parts of the spectrum, but it cannot recover the lost part of it. In effect we get an ideal low pass filtering of the test pattern, which corresponds well with the peaky nature of deconvoluted curve in Figure 7.

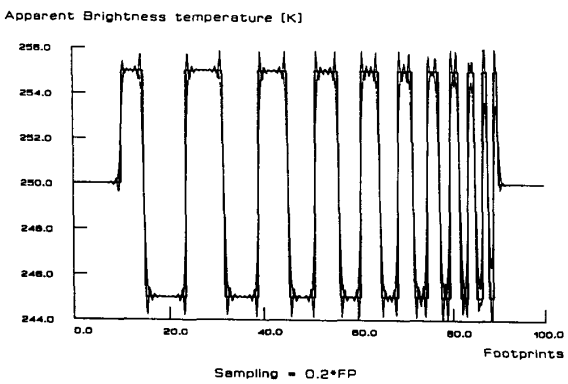

Figure 7: Deconvolution, ΔT=0.0 K

The quality of the deconvolution can be expressed quantitatively as follows: taking all points in the scene (Figure 7) the standard deviation between the test pattern and the pattern after convolution is 1.407 K. The standard deviation between the test pattern and the deconvoluted pattern is 1.030 K, i. e. some improvement is present.

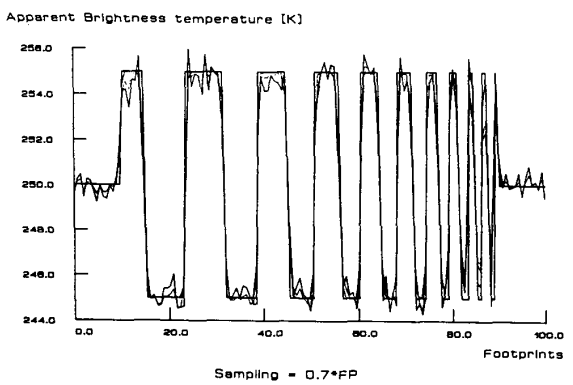

Figure 8: Deconvolution, ΔT=0.25 K

The real problems with deconvolution arise when radiometric noise is present. **Figure 8** shows results with ΔT=0.25 K. The noisy curve with the largest spikes is the result after deconvolution, the other noisy curve is the result just before deconvolution. Again deconvolution improves the ability to follow the steep jumps in the test scene - but noise amplification is clearly present: in the flat parts of the pattern the resulting ΔT is worse than before deconvolution.

The deconvolution process requires some assumptions about the spectrum of the original input scene. In Figure 8 the process is optimized for the scene, and an improvement in the standard deviation of some 0.2 K is found despite the noise amplification. If we assume that the scene continues in a much smoother fashion where the antenna response is fast enough to follow the variations, and the deconvolution is left unchanged, the noise amplification vill seriously degrade the radiometric resolution over this area. Hence, it can be concluded that shall deconvolution be applied to the output of an imaging radiometer system, it must be adaptive.

ACKNOWLEDGEMENT

This work was carried out with support from the European Space Agency through its research and technology centre, ESTEC.

REFERENCES

[1] Ulaby, F. T., Moore, R. K., and Fung, A. K., "Microwave Remote Sensing - Vol. 1", Artech House, 1981

[2] Skou, N., "Microwave Radiometer Systems. Analysis & Design", Artech House, 1989.

[3] Evans, G., McLeish, C. W., "RF Radiometer Handbook", Artech House, 1977.

[4] Rosenkrantz, P. W., "Inversion of Data from Diffraction Limited Multiwavelength Remote Sensors, 1, Linear Case", Radio Science, Vol. 13, No. 6, pp 1003 - 1010, November-December 1978.

[5] Reyneri, L. M., Nesti, G., "Optimization of Scan Parameters and Post-Detection Filter Parameters for a Passive Microwave Sensor", in "Microwave Radiometry and Remote Sensing Applications", ed. P. Pampaloni, VSP, 1989.